Dual-color total internal reflection fluorescence cross-correlation spectroscopy

Marcel Leutenegger,[a,*] Hans Blom,[b] Jerker Widengren,[b] Christian Eggeling,[c] Michael Gösch,[a] Rainer A. Leitgeb,[a] and Theo Lasser[a]

[a]Laboratoire d'Optique Biomédicale
École Polytechnique Fédérale de Lausanne
1015 Lausanne, Switzerland
[b]Biomolekylär Fysik
Kungliga Tekniska Högskolan
10691 Stockholm, Sweden
[c]Max-Planck-Institut für Biophysikalische Chemie
37077 Göttingen, Germany

Abstract. We present the development and first application of a novel dual-color total internal reflection (TIR) fluorescence system for single-molecule coincidence analysis and fluorescence cross-correlation spectroscopy (FCCS). As a performance analysis, we measured a synthetic DNA-binding assay, demonstrating this dual-color TIR-FCCS approach to be a suitable method for measuring coincidence assays such as biochemical binding, fusion, or signal transduction at solid/liquid interfaces. Due to the very high numerical aperture of the epi-illumination configuration, our setup provides a very high fluorescence collection efficiency resulting in a two- to three-fold increase in molecular brightness compared to conventional confocal FCCS. Further improvements have been achieved through global analysis of the spectroscopic data. [DOI: 10.1117/1.2221714]

Keywords: fluorescence spectroscopy; laser-induced fluorescence; correlation.

Paper 06008LR received Jan. 17, 2006; revised manuscript received Apr. 12, 2006; accepted for publication May 26, 2006; published online Jul. 11, 2006.

Total internal reflection fluorescence microscopy (TIR-FM) is an important tool in life science. Taking advantage of a very thin (<100 nm) optical excitation depth formed by an evanescent wave above a glass substrate, TIR fluorescence detection achieves an exceptional axial resolution and allows for the study of important cellular processes, in particular at or near the cellular membrane.[1] Prominent biological applications of TIR-FM include real-time *in vivo* observations of dynamics of molecular motors,[2,3] or of various membrane trafficking events, such as vesicle fusion or signal transduction after receptor binding.[4,5] To extend the sensitivity and observation of such cellular assays, it is important to combine TIR-FM with fluorescence measurement and single-molecule fluctuation analysis. Fluorescence correlation spectroscopy enables to expose biological reactivity such as binding events on the basis of temporal fluctuations in the fluorescence emission of single molecules.[6,7] Dual-color fluorescence cross-correlation spectroscopy (FCCS) represents a further development of fluctuation spectroscopy, which achieves a significantly improved selectivity and applicability.[8] FCCS institutes two differently colored labels and realizes the distinction between coinciding and separated occurrence of these labels. It thus introduces a useful tool to monitor various biological assays including molecular binding between two differently labeled binding partners. Typically, FCCS is based on a confocal epi-illumination microscope with multicolor laser excitation and single-photon detection. Nonetheless, for several applications, TIR illumination can provide further benefits, for instance when ligands interacting with receptors immobilized onto a surface are to be studied.[9–12] First, in TIR-FCCS the molecules are only excited near the glass-sample interface, which simplifies the discrimination between freely diffusing and immobilized particles. Second, the most important prerequisite for efficient single-molecule detection is a high fluorescence count rate per molecule (CPM). Using TIR excitation and exploiting the anisotropic emission of the fluorescence generated at the glass-sample interface, much higher CPM can be extracted from the investigated molecules.[13]

In this work, we present for the first time a dual-color excitation scheme for TIR single-molecule detection, which enables us to perform FCCS at glass-sample interfaces with high sensitivity. The improved performance of TIR-FCCS was verified on a synthetic binding assay, including dual-labeled double-stranded DNA molecules in aqueous solution, demonstrating its potential for biological and cellular applications.

Figure 1 shows our dual-color TIR-FCCS setup. Two linear polarized laser beams were expanded to an e^{-2} diameter of $\approx$2 mm and collinearly aligned to the microscope objective (BE & BS; beam expansion 2.5×). The laser powers were controlled by neutral density filters. An achromatic lens focused the beams into the back-focal plane (BFP) of the high numerical aperture (NA) oil immersion objective (α-Plan-Fluar 100×1.45 with Immersoil™ 518F, Carl Zeiss Jena, Jena, Germany), which resulted in circular spots with e^{-2} diameters at the cover slide-sample interface of $\approx$16 μm (blue) and $\approx$20 μm (red), respectively. In the BFP, a beam foci offset of $\approx$2.3 mm from the optical axis resulted in a super-critical angle illumination, i.e., a z-confinement below 100 nm resulting from the evanescent field excitation.

Due to the epi-illumination, the fluorescent light was collected with the same high NA objective toward the pinholes and the single-photon detectors. The pinholes were realized by two multimode fibers with a core diameter of 50 μm. Dichroic mirrors and bandpass filters blocked the back-reflected laser light by more than OD10 and provided an excellent filtering of the green and red fluorescence. The fluorescence photons were detected by fiber-coupled single photon counting modules (SPCM-AQR-14-FC, PerkinElmer Optoelectronics, Wiesbaden, Germany; ASY50/105 silica fibers, Thorlabs Inc., Grünberg, Germany), whose signals (number of photons over time) were recorded and correlated with a USB hardware correlator (Flex02-08D, Correlator.com, Bridgewater, New Jersey). A focusing lens, a $\lambda/4$ plate, and a dichroic mirror were moved in one block by a linear translator for adjusting the position of the beam foci in the BFP of the objective. In this way, the excitation angle could be adjusted without alter-

*Tel: +41 21 693 78 21; E-mail: marcel.leutenegger@epfl.ch

1083-3668/2006/11(4)/040502/3/$22.00 © 2006 SPIE

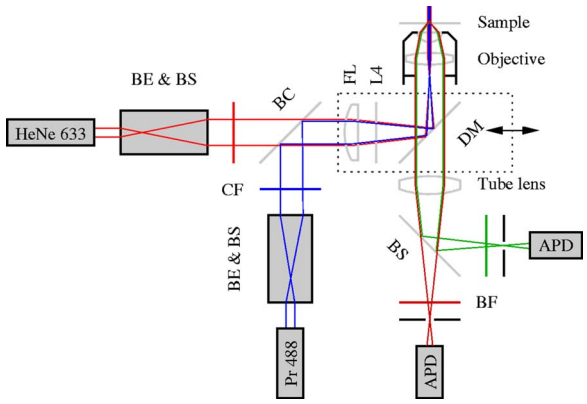

Fig. 1 Dual-color TIR-FCCS setup. HeNe 633: 18-mW HeNe gas laser (LHRP-1701, Laser 2000, Weßling, Germany). Pr 488: 22-mW solid-state laser (Protera™ 488-15, Novalux, Sunnyvale, CA). BE & BS: 2.5× beam expanders and beam steerers. CF: laser-line cleanup filters [Chroma Z488/10x (blue); Chroma Z633/10x (red); Chroma Technology Corp., Brattleboro, VT]. BC: dichroic beam combiner (Chroma Z488bcm). FL: focusing lens (achromat f=130 mm). L4: λ/4 plate oriented for maximum fluorescence (OWIS, Staufen, Germany). DM: dual-band dichroic mirror (Omega DM488/633, Omega Optical Inc., Brattleboro, VT). Sample: droplet on a 150-μm-thick glass cover slide mounted on a xyz-translation stage (ULTRAlign 561D with μDrive Controller ESA-C, Newport Corp., Darmstadt, Germany). BS: dichroic beam splitter (Omega DML625). BF: emission band-pass filters [Chroma HQ540/80m and Omega 520DF40 (green); Chroma HQ690/80m and Omega 685DF70 (red)]. APD: detectors (Color online).

ing the optical path length between the focusing lens and the objective. The configuration can easily be changed to a conventional confocal epi-illumination by removing the focusing lens and by centering the collimated beams in the BFP.

As a synthetic binding assay, we used free rhodamine green (RhG) and Cy5 fluophores, and a 40 base pair double-stranded DNA labeled with Alexa488 and Cy5 (Zeiss cross-correlation standard). The laser powers were optimized with the dsDNA sample and the background was measured with a NaCl/EDTA/TRIS pH 8.0 buffer. The cross talk between the detection channels was calibrated with free 10-nM RhG and 50-nM Cy5, respectively. For cross-correlation measurements, different mixtures of the double-labeled dsDNA

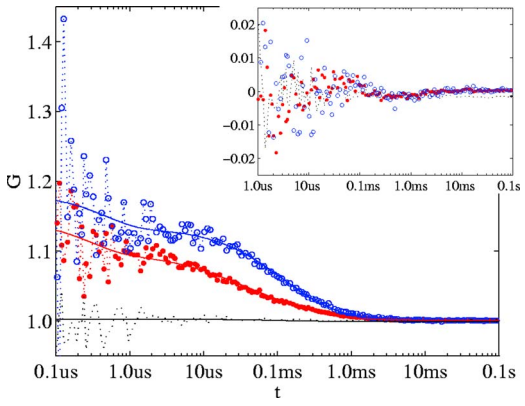

Fig. 2 Negative control (9-nM RhG/50-nM Cy5). Circles: green autocorrelation. Bold points: red autocorrelation. Dots: green-red cross-correlation. Inset: fit residuals $G_{\text{fit}}/G_{(\tau)}-1$ (Color online).

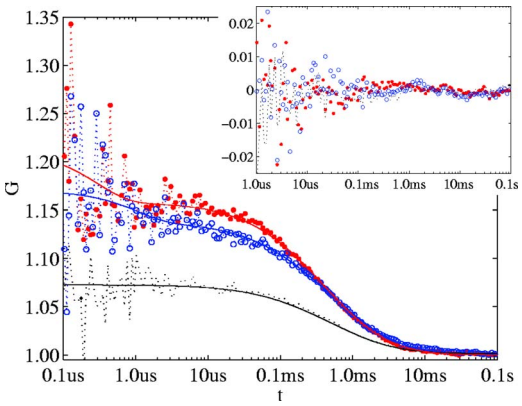

Fig. 3 Positive control (dsDNA). Circles: green autocorrelation. Bold points: red autocorrelation. Dots: green-red cross-correlation. Inset: fit residuals (Color online).

sample and free 9-nM RhG/50-nM Cy5 solutions were used and investigated with identical laser powers during a time interval of 20 s. Plasma cleaning of the cover slides improved the results due to a strong suppression of unspecific binding at the glass surface.

For free diffusion the following model equation was used:[13]

$$G_{mn(\tau)} = G_{mn\infty} + \frac{1}{2}\left(1 - \frac{B_m}{I_m}\right)\left(1 - \frac{B_n}{I_n}\right)\frac{\sum Q_{mi}Q_{ni}N_iD_{mni(\tau)}}{\sum Q_{mi}N_i \sum Q_{ni}N_i} + G_{mnt}\exp\left(-\frac{\tau}{\tau_{mnt}}\right).$$

Here, indices m and n represent the green and red detection channels; hence G_{gg} and G_{rr} are the autocorrelations of the signals in the green and red detection channels, respectively, and G_{gr} is the cross-correlation of both signals. The index i represents the diffusing species: g for RhG, r for Cy5, and c for the dsDNA. Also, B is the measured background count rate, I is the total count rate, Q_{mi} is the CPM in channel m of species i, N_i are the number of molecules in the effective sampling volume, G_{mnt} and τ_{mnt} are the triplet amplitudes and the triplet correlation times, respectively, $G_{mn\infty} \approx 1$ are the offsets at infinite lag time τ, and D_{mni} describes the diffusion and is given by[13]

$$D_{mni(\tau)} = \left(1 + \frac{\tau}{\tau_{ixy}}\right)^{-1}\left[\sqrt{\frac{\tau}{\pi\tau_{iz}}} + \left(1 - \frac{\tau}{2\tau_{iz}}\right)\text{erfcx}\left(\sqrt{\frac{\tau}{4\tau_{iz}}}\right)\right]$$

where τ_{iz} and τ_{ixy} are the axial and lateral diffusion times of species i, respectively, and the scaled complementary error function is $\text{erfcx}(x) = \exp(x^2) \times \text{erfc}(x)$. A multidimensional least-squares Gaussian-Newtonion algorithm was used to fit the experimental data to these model equations.

For these first experiments, only relative concentrations of the species were of interest. Therefore, a unique diffusion time was used, neglecting channel differences due to an imperfect overlap of the excitation and detection volumes. The triplet term accounts for the triplet contribution in the initial correlation amplitude $G_{(0)}$.

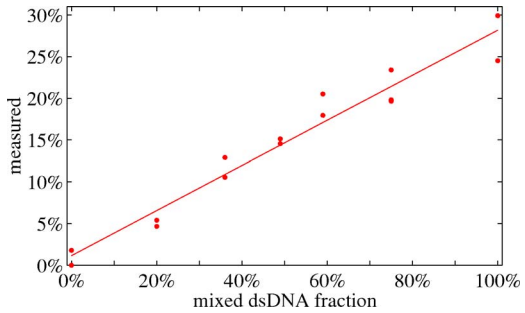

Fig. 4 Measured fraction of dsDNA versus mixed fraction

The measured background signals were $B_g=7.54$ kHz and $B_r=19.6$ kHz, respectively. Typically, autofluorescence from the immersion oil as well as from the glass slide were the main contributions to B_g and B_r, respectively. The crosstalk CPM of RhG in the red channel was found to be $Q_{rg}=0.032\times Q_{gg}$ and assumed constant during the following evaluations. Cy5 did not show any crosstalk in the green channel, hence $Q_{gr}=0$. Therefore, the CPM were replaced by the crosstalk factor $Q_{rg}/Q_{gg}=0.032$ for simplification.

Figure 2 shows the correlation results for a mixture of the free fluorophores (negative control). The count rates of this control sample were $I_g=40.2$ kHz and $I_r=66.0$ kHz. The CPMs were $Q_{gg}=(I_g-B_g)/N_g=13.1$ kHz and $Q_{rr}=[I_r-B_r-0.032\times(I_g-B_g)]/N_r=18.9$ kHz, respectively. Figure 3 shows the results for the Cy5 and Alexa488 labeled dsDNA correlation (positive control). We measured $I_g=39.3$ kHz and $I_r=44.2$ kHz, from which $Q_{gc}=13.3$ kHz and $Q_{rc}=27.0$ kHz were extracted. The increased count rate for bound Cy5 is attributed to a reduction of conformational changes leading to higher fluorescence emission.[14,15] For $\tau>10$ μs, the fit residuals were lower than 10^{-2}. For smaller lag times, shot noise and afterpulsing reduced the signal-to-noise ratio.

Figure 4 summarizes the TIR-FCCS measurements on a titration series of double-labeled dsDNA in a mixture of free 9-nM RhG/50-nM Cy5, such that the total fluorophore concentration was approximately constant. The measured fraction of dsDNA scaled linearly with the mixed fraction from ≈1% (negative control) to ≈28% (positive control). The measurements showed a relative scatter of ≈±15%. The measured fraction was at best one-third of the mixed fraction. This can be explained by an excess of molecules with a single green label, possibly further enhanced by photobleaching of the red label during the two-color excitation.[15] The overlap of the sampling volumes was estimated to ≈60%, which is close to the theoretical maximum. To reduce the influence of photobleaching, we used excitation intensities of ≈10 $\mu W/\mu m^2$. The measured CPM were about two times higher than with a confocal epi-illumination and a 1.20 NA water immersion objective at identical excitation intensities.[13,16]

The diffusion times of the dsDNA were $\tau_z=51$ μs axially and $\tau_{xy}=2.3$ ms laterally, respectively. Given a penetration depth of 80 nm and a waist radius of 370 nm, the diffusion constant was calculated to $D\approx 1.5\times 10^{-7}$ cm^2/s, which is about 22% of the estimation $D_{DNA}\approx 6.8\times 10^{-7}$ cm^2/s for a rodlike molecule with a diameter of 24 Å and a length of 140 Å. We attribute this to an increased hydrodynamic drag near the interface and weak unspecific binding, respectively.

This study demonstrates for the first time single-molecule FCCS measurements based on an epi-illumination TIR concept. This TIR-FCCS concept offers distinct advantages to confocal FCCS for coincidence assays at solid/liquid surfaces, in particular by virtue of the much higher fluorescence collection efficiencies and the confinement of the excitation field to the surface of interest.

Acknowledgments

We thank Aram Mooradian of Novalux for the Protera laser and his continous interest in our work, Klaus Weisshart of Carl Zeiss for contributing the cross-correlation sample, and Kai Hassler and Rudolf Rigler for many expert discussions. This work was supported by the Swiss National Science Foundation (SNSF) Grant No. 200021-103333. Jerker Widengren acknowledges support from the Swedish Strategic Research Foundation (SSF, BioX).

References

1. D. Axelrod, "Total internal reflection fluorescence microscopy in cell biology," *Traffic (Oxford, U. K.)* **2**, 764–774 (2001).
2. Y. Sako and T. Uyemura, "Fluorescence correlation spectroscopy with single-molecule sensitivity on cell and model membranes," *Cell Struct. Funct* **27**, 357–365 (2002).
3. Y. Sako and T. Yanagida, "Single-molecule visualization in cell biology," *Nat. Rev. Mol. Cell Biol.* **4**, SS1-SS5 (2003).
4. D. Toomre and D. J. Manstein, "Lighting up the cell surface with evanescent wave microscopy," *Trends Cell Biol.* **11**, 298–303 (2001).
5. V. Beaumont, "Visualizing membrane trafficking using total internal reflection fluorescence microscopy," *Biochem. Soc. Trans.* **31**, 819–823 (2003).
6. R. Rigler, Ü. Mets, J. Widengren, and P. Kask, "Fluorescence correlation spectroscopy with high count rate and low background - Analysis of translational diffusion," *Eur. Biophys. J.* **22**, 169–175 (1993).
7. S. Weiss, "Fluorescence spectroscopy of single biomolecules," *Science* **283**, 1676–1683 (1999).
8. K. Bacia, I. V. Majoul, and P. Schwille, "Probing the endocytic pathway in live cells using dual-color fluorescence cross-correlation analysis," *Biophys. J.* **83**, 1184–1193 (2002).
9. A. M. Lieto, R. C. Cush, and N. L. Thompson, "Ligand-receptor kinetics measured by total internal reflection with fluorescence correlation spectroscopy," *Biophys. J.* **85**, 3294–3302 (2003).
10. P. Schwille, J. Korlach, and W. W. Webb, "Fluorescence correlation spectroscopy with single-molecule sensitivity on cell and model membranes," *Cytometry* **36**, 176–182 (1999).
11. R. L. Hansen and J. M. Harris, "Measuring reversible adsorption kinetics of small molecules at solid/liquid interfaces by total internal reflection fluorescence correlation spectroscopy," *Anal. Chem.* **70**, 4247–4256 (1998).
12. N. L. Thompson, T. P. Burghardt, and D. Axelrod, "Measuring surface dynamics of biomolecules by total internal-reflection fluorescence with photobleaching recovery or correlation spectroscopy," *Biophys. J.* **33**, 435–454 (1981).
13. K. Hassler, M. Leutenegger, P. Rigler, R. Rao, R. Rigler, M. Gösch, and T. Lasser, "Total internal reflection fluorescence correlation spectroscopy (TIR-FCS) with low background and high count-rate per molecule," *Opt. Express* **13**, 7415–7423 (2005).
14. J. Widengren and P. Schwille, "Characterization of photoinduced isomerization and back-isomerization of the cyanine dye Cy5 by fluorescence correlation spectroscopy," *J. Phys. Chem. A* **104**, 6416–6428 (2000).
15. C. Eggeling, J. Widengren, L. Brand, J. Schaffer, S. Felekyan, and C. A. M. Seidel, "Analysis of photobleaching in single-molecule multicolor excitation and Förster resonance energy transfer measurements," *J. Phys. Chem. A* **110**, 2979–2995 (2006).
16. J. Mertz, "Radiative absorption, fluorescence, and scattering of a classical dipole near a lossless interface: a unified description," *J. Opt. Soc. Am. B* **17**, 1906–1913 (2000).